GEOLOGY | THE GEOLOGICAL SOCIETY OF AMERICA®

https://doi.org/10.1130/G49637.1

Manuscript received 28 August 2021
Revised manuscript received 15 December 2021
Manuscript accepted 21 December 2021

Published online 8 March 2022

Linking metamorphism and plate boundaries over the past 2 billion years

Yebo Liu[1], Ross N. Mitchell[2]*, Michael Brown[3], Tim E. Johnson[1] and Sergei Pisarevsky[1,4]

[1]Earth Dynamics Research Group, The Institute for Geoscience Research (TIGeR), Department of Earth and Planetary Sciences, Curtin University, GPO Box U1987, Perth, WA 6845, Australia

[2]State Key Laboratory of Lithospheric Evolution, Institute of Geology and Geophysics, Chinese Academy of Sciences, Beijing 100029, China

[3]Laboratory for Crustal Petrology, Department of Geology, University of Maryland, College Park, Maryland 20742, USA

[4]Institute of the Earth's Crust, Siberian Branch of the Russian Academy of Sciences, Irkutsk 664033, Russia

ABSTRACT

Since the Jurassic, there has been a clear spatiotemporal correlation between different types of metamorphism and active convergent plate margins. However, the extent to which this relationship extends into the past is poorly understood. We compared paleogeographic reconstructions and inferred plate kinematics with the age and thermobaric ratio (temperature/pressure [*T/P*]) of metamorphism over the past 2 b.y. The null hypothesis—that there is no spatiotemporal link between inferred plate margins and metamorphism—can be rejected. Low-*T/P* metamorphism is almost exclusively located near plate margins, whereas intermediate- and high-*T/P* metamorphism skews toward increasingly greater distances from these margins, consistent with three different tectonic settings: the subduction zone, the mountain belt, and the orogenic hinterland, respectively. However, paleogeographic reconstructions suggest that so-called "paired metamorphic belts" are rare and that high- and low-*T/P* localities more commonly occur along strike from each other. The observation that bimodal metamorphism is largely a function of distance from the trench and that end-member *T/P* types rarely occur in the same place can be explained if the style of orogenesis has evolved from hotter to colder, consistent with the abrupt emergence of low-*T/P* metamorphism in the Cryogenian. The widespread development of high-*T/P* rocks in orogenic hinterlands in the Proterozoic was followed by the production and efficient exhumation of low-*T/P* rocks in subduction channels in the Phanerozoic.

INTRODUCTION

Using the thermobaric ratio (temperature/pressure [*T/P*]), metamorphism has been classified into three types (Fig. 1; Brown, 2007; Brown and Johnson, 2019a, 2019b): high-*T/P* metamorphism ($T/P > 775$ °C GPa^{-1}), intermediate-*T/P* metamorphism ($T/P = 775$–375 °C GPa^{-1}), and low-*T/P* metamorphism ($T/P < 375$ °C GPa^{-1}). On contemporary Earth, each type of metamorphism generally occurs in a particular tectonic setting associated with subduction-to-collision orogenesis (Brown, 2010). Low-*T/P* metamorphism, characterized by blueschists, low-temperature (quartz) eclogites, and ultrahigh-pressure (coesite/diamond) eclogites, forms in subduction channels associated with accretionary orogens and during partial subduction of passive continental margins. Intermediate-*T/P* metamorphism, characterized by high-*P* granulites and medium- to high-*T* eclogites, is generally associated with the thickened orogenic core and mountain belts. High-*T/P* metamorphism, characterized by upper-amphibolite-facies and granulite-facies (including ultrahigh-temperature) rocks, occurs in orogenic hinterlands (back-arcs and plateaus).

The strong temporal clustering of metamorphic occurrences during periods of supercontinent assembly is well established (Brown, 2007). However, although a close spatial association between metamorphism and convergent plate margins is assumed to hold into the geological past (Brown and Johnson, 2019a; Chowdhury et al., 2020), this assumption has not been tested. We investigated how specific styles of metamorphism relate to plate kinematics by coupling metamorphic *T/P* data with continental reconstructions over the past 2 b.y.

METHOD

We used the metamorphic database of Brown and Johnson (2019b), which includes geographic locations (Table S1 in the Supplemental Material[1]). The data were plotted as stacked histograms according to *T/P* type and location as a function of the distance from an inferred plate margin (Fig. 1A) and age (Fig. 1B).

Here, "plate margin" refers to the continental edge closest to the metamorphic locality as a proxy for the location of the nearest convergent plate boundary, although in reality, the trench may have been tens of kilometers from this margin, particularly earlier in Earth history. Although plate-boundary topologies can be plotted in reconstructions based on inferences from the geologic record over the past billion years (Merdith et al., 2021), such efforts are in their infancy. Notwithstanding these factors, for completeness, we also calculated the distance of metamorphic localities from modeled topological boundaries (Merdith et al., 2021) over the past 1 b.y. (Fig. S9). This approach results in a median value of 405 km from a plate boundary, possibly due to an oversimplification of plate boundaries that is avoided in our preferred approach.

In our study, reconstructions for 2200–600 Ma were taken from Li et al. (2019), and those in the Phanerozoic were taken from

*E-mail: ross.mitchell@mail.iggcas.ac.cn

[1]Supplemental Material. Methods, ten supplemental figures, one supplemental table, and references. Please visit https://doi.org/10.1130/GEOL.S.19104980 to access the supplemental material, and contact editing@geosociety.org with any questions.

CITATION: Liu, Y., Mitchell, R.N., Brown, M., Johnson, T.E., and Pisarevsky, S., 2022, Linking metamorphism and plate boundaries over the past 2 billion years: Geology, v. 50, p. 631–635, https://doi.org/10.1130/G49637.1

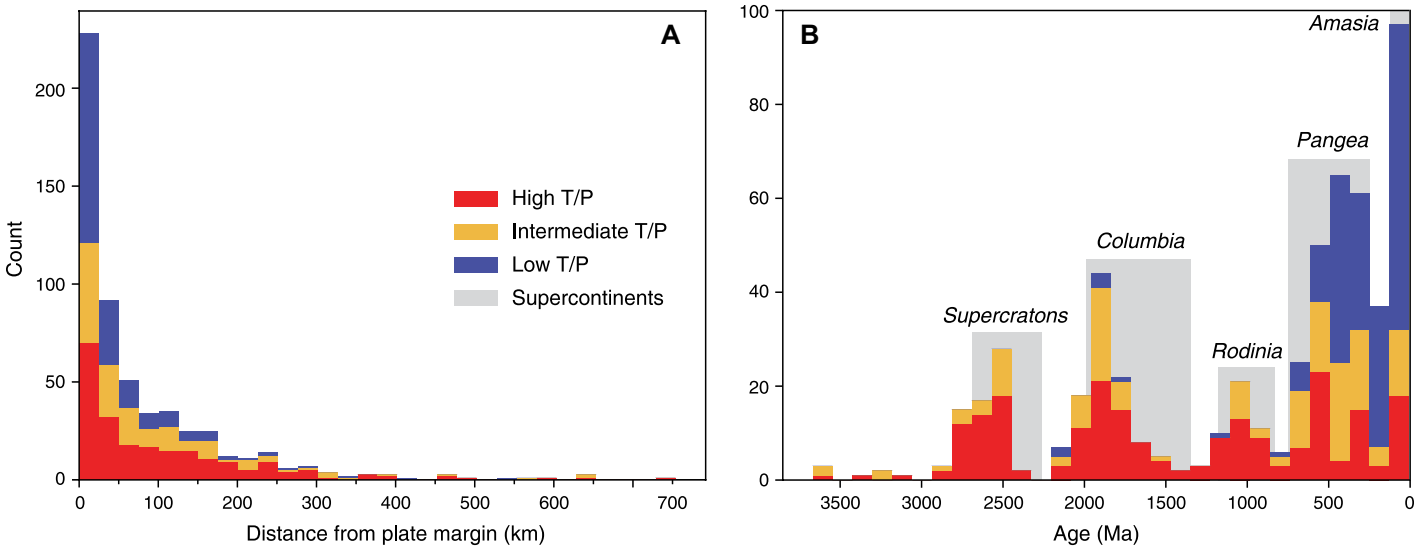

Figure 1. Histograms of spatiotemporal data for metamorphic occurrences. (A) Stacked histogram of distance of metamorphic occurrences from nearest inferred plate margin. Detailed methods and results are provided in Supplemental Material (see footnote 1). (B) Stacked histogram of ages of metamorphic occurrences through time. Durations of supercontinents from Mitchell et al. (2021) were vertically scaled to data in front of them so as not to distract from peak heights. Data in both panels are color-coded according to thermobaric ratio (temperature/pressure [*T/P*]) type.

Matthews et al. (2016). Series of maps showing metamorphic occurrences in paleogeographic reconstructions, along with the best estimate of distance from the nearest cratonic or continental margin at that time, are presented in Figures S1–S8. Detailed methods are also provided in the Supplemental Material.

TESTS OF NULL HYPOTHESES

Metamorphism and Plate Boundaries

We first tested the null hypothesis that there is no association between plate boundaries and metamorphism. If the null hypothesis is true, then for any given age range, the distances of metamorphic localities should be randomly distributed, with as many localities away from plate boundaries as are close to them. A histogram of metamorphic localities (Table S1) in terms of distance from a plate margin is shown in Figure 1A. Based on the average width of contemporary arc systems (~80–240 km; England, 2018), we used a distance of 150 km as a reasonable maximum for classifying metamorphism at that locality as being spatially related to a convergent plate boundary.

Of the metamorphic localities, 83% (466/564) occur near plate margins, with the remaining 17% interpreted to represent intraplate metamorphism. Adjusting the cutoff distance from a plate margin to 100 km or to 50 km still results in a majority of localities (72% and 57%, respectively) located near plate margins. Taken as a whole, the *T/P* data show a skewed distribution (Fig. 1A), indicating that metamorphism mostly occurs close to plate margins, but it becomes increasingly rare farther away. Thus, the first null hypothesis is rejected.

Type of Metamorphism and Distance from Plate Boundaries

We then tested the null hypothesis that there is no relationship between the type of metamorphism (in terms of *T/P*) and distance from the inferred plate boundary. Our analysis of distance from plate margins (plotted on a log-scale due to the skewness) by metamorphic type revealed striking differences (Fig. 2). The distributions for low- and high-*T/P* metamorphism are themselves skewed, with low-*T/P* locations (median = 15 km) closer to plate margins and high-*T/P* occurrences (median = 62 km) some four times more distant. The distribution for intermediate-*T/P* metamorphism is normally distributed without skewness and defines an intermediate median distance of 45 km from an inferred plate boundary. Considering the likelihood for postmetamorphic orogenic contraction and strike-slip translation, the distributions of distance from a plate margin for low-, intermediate-, and high-*T/P* localities are consistent with metamorphism in a subduction channel, in a mountain belt, and in an orogenic hinterland, respectively. As the contrasting distributions defined by the data from each *T/P* type sample different populations, we reject the second null hypothesis.

Distribution of Types of Metamorphism Along Plate Boundaries

Next, we tested a third null hypothesis that there is no spatial relationship between low-*T/P* and high-*T/P* metamorphism along any single plate boundary. The western North American Cordillera (Fig. 3A) records dominantly high-*T/P* metamorphism, with only one low-*T/P* locality (associated with an accreted terrane), whereas farther around the Pacific "Ring of Fire," low-*T/P* metamorphism becomes increasingly dominant. Only in Japan are high- and low-*T/P* metamorphism collocated, and in this case, the two metamorphic belts were tectonically juxtaposed (Brown, 2010).

The Tethys orogenic system (Fig. 3A) also exhibits along-strike variation in *T/P* type: low-*T/P* metamorphism is exclusively developed along its western extent in the Alps, whereas intermediate-*T/P* metamorphism dominates the eastern Himalayan syntaxis, with only rare instances of high-*T/P* metamorphism. Changes along strike from west to east likely relate to a number of factors in addition to differences between accretionary and collisional orogens, for example, evolution from a small cold to a large hot orogen (Jamieson and Beaumont, 2013). Although different, in both these modern cases of accretionary and collisional orogens, we are able to reject the third null hypothesis, since there is a relationship whereby at least some localities with contrasting *T/P* occur along the same plate boundaries or orogenic systems.

Type of Metamorphism and Paleolatitude

Finally, using paleogeographic reconstructions, we tested the hypothesis that exhumation of low-*T/P* terranes was limited to low latitudes; in particular, ultrahigh-pressure (UHP) low-*T/P* metamorphic terranes, as proposed by Yan and Zhang (2019). As continuous reconstructions are only available for the past 1 b.y., this test was restricted to metamorphic data from rocks younger than 1 Ga (Figs. S4–S8). As the distributions of paleolatitude data from all three *T/P* types are essentially uniform (Fig. 4), the null hypothesis that there is no relationship between *T/P* type

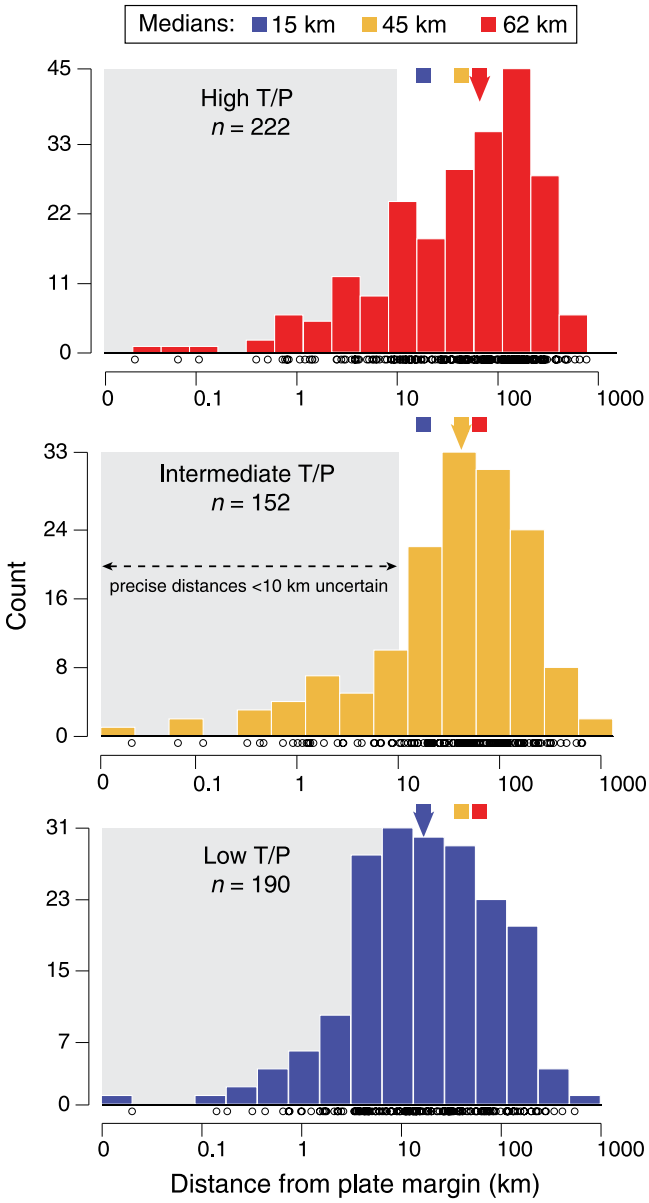

Figure 2. Histograms of distance of metamorphic localities from plate margin by thermobaric ratio (temperature/pressure [*T*/*P*]) type.

and latitude cannot be rejected. However, the hypothesis that exhumation of low-*T*/*P* metamorphic terranes was limited to low latitudes is falsified by our data.

PALEOGEOGRAPHIC CONTEXT

Amasia (200 Ma to Present)

The assembly of the next supercontinent, Amasia, is already under way with the ongoing formation of the Eurasian megacontinent that began ca. 250 Ma (Wang et al., 2021). In Amasia, orogens related to the rifting, transfer, and collision of continental terranes from Gondwana to Eurasia have been accommodated by the Tethys orogenic system (Wan et al., 2019). Although all three types of metamorphism are present, Tethyan orogens are dominated by low-*T*/*P* metamorphism (Fig. 3A). Moreover, with one exception in Turkey, the western sector of the Tethyan orogenic system records exclusively low-*T*/*P* metamorphism. Occurring at much greater distances from a margin, the high-*T*/*P* metamorphism recorded by the Cordilleran localities is consistent with their continental backarc setting (Hyndman et al., 2005).

Pangea (850–200 Ma)

The Pangea supercontinent cycle extended from the early formation of the Gondwana megacontinent between ca. 850 and 520 Ma to complete assembly of Pangea by ca. 350 Ma and its initial breakup at ca. 200 Ma. Although the data are limited, early Gondwanan orogenesis during the late Neoproterozoic (Fig. S5) was associated with all three types of metamorphism, whereas the suturing of Pan-African orogens that continued into the early Paleozoic (Fig. S6) defined a large area recording dominantly high-*T*/*P* metamorphism in central Gondwana (Fig. 3B). By contrast, in the mid-Paleozoic, rocks in the Caledonian collisional belt recorded dominantly intermediate- and low-*T*/*P* metamorphism, although high-*T*/*P* metamorphism occurred farther south along the Acadian margin of Laurentia (Fig. 3B).

The Caledonian orogen is notably asymmetric, with dominantly low-*T*/*P* metamorphism on the Baltica side of the suture and dominantly intermediate-*T*/*P* metamorphism on the Laurentia side (Fig. S6). Arc magmatism in East Greenland indicates the subduction polarity, with Laurentia as the upper plate and Baltica as the lower (subducted) plate (Augland et al., 2012). Finally, in the late Paleozoic, the Alleghenian/Variscan orogenic system recorded closure of the Rheic Ocean during collision between Cadomian terranes and Laurussia (Fig. 3B). Early low-*T*/*P* metamorphism occurred in the Baltican segment of the orogen (Fig. S7), with younger intermediate- and high-*T*/*P* metamorphism developing along the length of the final suture. However, there is no record of low-*T*/*P* metamorphism during the final suturing of Pangea. Thus, the apparent spatial pattern of dominantly high-*T*/*P* metamorphism in the south and dominantly low-*T*/*P* metamorphism in the northern parts of Pangea (Fig. 3B) likely reflects diachronous assembly.

Rodinia (1350–850 Ma)

The Grenville orogen *sensu stricto*, including the eastern margin of Laurentia and its immediate neighbors (e.g., Baltica and Amazonia; Martin et al., 2020), is largely characterized by intermediate- and high-*T*/*P* metamorphism, with only one low-*T*/*P* locality (Fig. 3C). High-*T*/*P* metamorphism also dominates in the Kalahari (southern Africa), Australia, and greater India, which may represent the along-strike continuation of the larger Grenvillian-aged orogenic system (Hoffman, 1991). The appreciable number of metamorphic occurrences calls into question the characterization of this period as one of orogenic quiescence (Tang et al., 2021). Nonetheless, the dominance of high-*T*/*P* metamorphism may be consistent with thinner crust (Tang et al., 2021) during hotter mid-Proterozoic orogenesis (Spencer et al., 2021). There are only two known cases of low-*T*/*P* metamorphism associated with Rodinia: one locality in Tarim (northwest China) that has recently been placed at the periphery of Rodinia (Zhao et al., 2021), and another in the Llano uplift (Texas, USA) in Laurentia. The dominance of a warmer (higher-*T*/*P*) type of orogenesis may reflect the double-sided subduction associated with collapse of the subduction girdle of accretionary orogens that formerly surrounded Columbia (Martin et al., 2020).

Columbia (2200–1350 Ma)

The record of Columbia (also known as Nuna) assembly (2.2–1.6 Ga) is preserved in

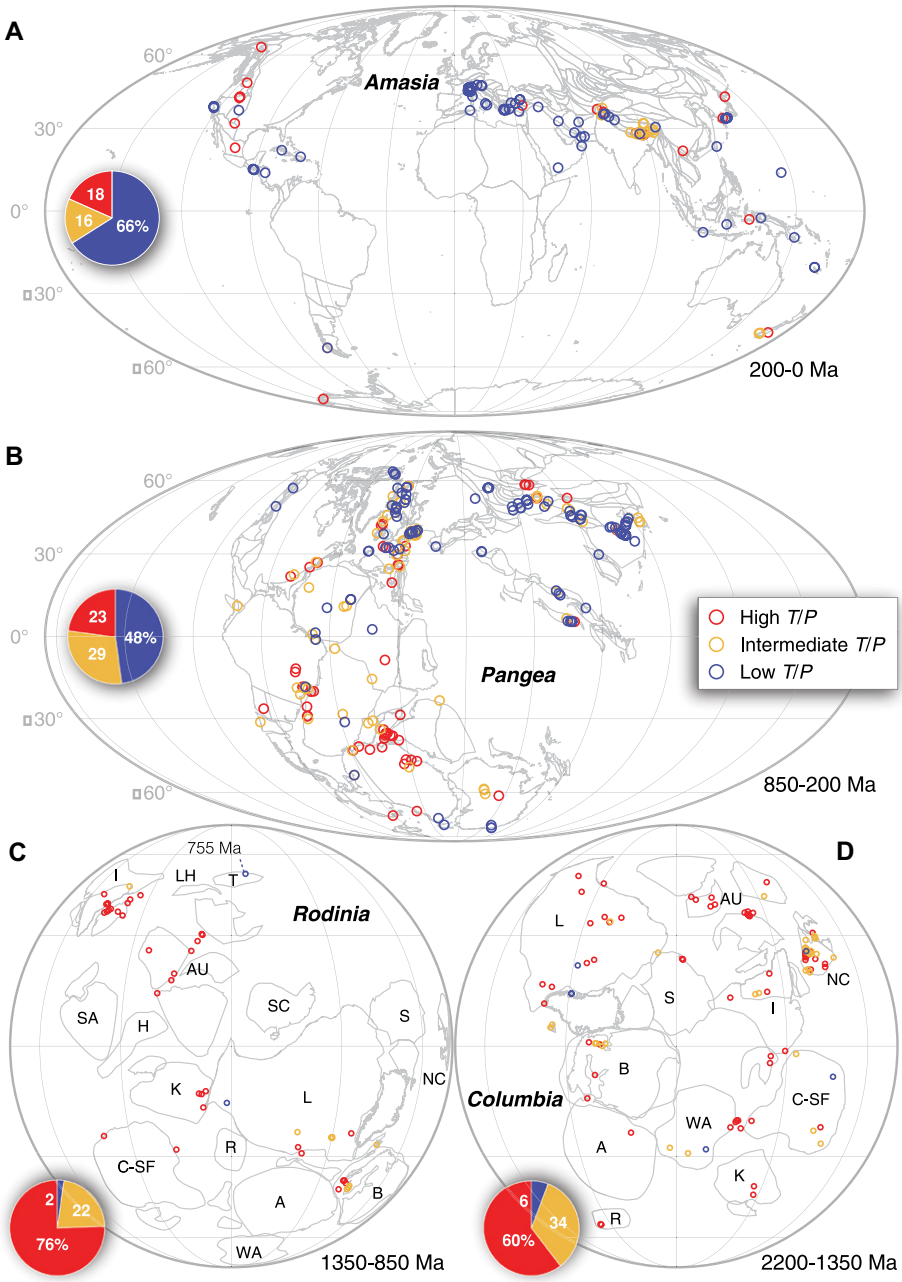

Figure 3. Paleogeographic maps of metamorphic occurrences. Data in all panels are color-coded according to thermobaric ratio (temperature/pressure [*T*/*P*]) type. Continent/craton abbreviations: A—Amazonia; AU—Australia; B—Baltica; C-SF—Congo-São Francisco; H—Hoggar; I—India; K—Kalahari; L—Laurentia; LH—Lhasa; NC—North China; R—Rio de la Plata; S—Siberia; SA—Sahara; SC—South China; T—Tarim; WA—West Africa. It should be noted that each map includes metamorphic data spanning a time interval, such that locations may be neither coeval in terms of age of peak metamorphism nor in these exact paleogeographic locations at time of metamorphism.

orogenic belts worldwide (Zhao et al., 2002) and arguably includes the period when Earth's subduction network became global (Wan et al., 2020) and plate tectonics *sensu stricto* began (Lenardic, 2018; Brown et al., 2020). Although dominated by high- and intermediate-*T*/*P* metamorphism, the assembly of Columbia is notable for the first occurrences of low-*T*/*P* metamorphism (Fig. 1B), all of which were located near the periphery of the supercontinent (Fig. 3D). With one exception, all occurrences younger than 1.6 Ga, which formed during the tenure and breakup of Columbia (Kirscher et al., 2021), are high-*T*/*P* rocks. As Australia already may have been fully formed (Liu et al., 2018), occurrences of high-*T*/*P* rocks during this time suggest intraplate metamorphism, although some argue that Australia may not have amalgamated until as late as ca 1.4–1.3 Ga (Gardiner et al., 2018).

IMPLICATIONS

Taken as a whole, the metamorphic *T*/*P* data show a clear bimodality since the Neoarchean, which has been interpreted to record the emergence of plate tectonics at some time during the Paleoproterozoic Era (Holder et al., 2019). Like those that formed in known tectonic settings as far back as the Jurassic, more ancient metamorphic rocks show a close spatial and temporal association with the inferred position of plate boundaries back to at least 2 Ga. Furthermore, our analysis lends support to the idea that the different types of metamorphism are related to distance from the plate margin and, thereby, to different tectonic settings—the trench (low *T*/*P*), the orogen (intermediate *T*/*P*), and the orogenic hinterland (high *T*/*P*) (Brown, 2007; Brown and Johnson, 2019a, 2019b). However, paleogeographic analysis shows that so-called "paired metamorphic belts" that juxtapose coeval low- and high-*T*/*P* metamorphism are rare.

The data show that mid-Proterozoic orogens (1850–850 Ma) spanning both Columbia and Rodinia were much warmer than more recent orogenic episodes (Fig. 3; Spencer et al., 2021). This can be explained if the style of orogenesis has evolved from warmer prior to the Cryogenian to colder since then. This transition may have been due to an increase in the supply of sediment to lubricate subduction zones following thawing of snowball Earth (Sobolev and Brown, 2019), allowing for production and subsequent exhumation of low-*T*/*P* rocks in subduction channels.

ACKNOWLEDGMENTS

This work was supported by grants from the National Natural Science Foundation of China (41888101 and 41890833) and the Chinese Academy of Sciences (IGGCAS201905) to R.N. Mitchell, and a Ministry of Science and Higher Education of the Russian Federation grant (075–15–2019–1883) to S.A. Pisarevsky. Y. Liu is supported by an Australian Research Council Laureate Fellowship grant to Z.X. Li (FL150100133). T.E. Johnson acknowledges support from the State Key Laboratory for Geological Processes and Mineral Resources, China University of Geosciences, Wuhan (Open Fund GPMR202101). We thank Damian Nance, Rob Strachan, and an anonymous reviewer for their insightful reviews. This is a contribution to International Geoscience Programme (IGCP) 648 (Supercontinent Cycles and Global Geodynamics) and Deep-time Digital Earth (DDE).

REFERENCES CITED

Augland, L.E., Andresen, A., Corfu, F., and Daviknes, H.K., 2012, Late Ordovician to Silurian ensialic magmatism in Liverpool Land, East Greenland: New evidence extending the northeastern branch of the continental Laurentian magmatic arc: Geological Magazine, v. 149, p. 561–577, https://doi.org/10.1017/S0016756811000781.

Brown, M., 2007, Metamorphic conditions in orogenic belts: A record of secular change: International Geology Review, v. 49, p. 193–234, https://doi.org/10.2747/0020-6814.49.3.193.

Brown, M., 2010, Paired metamorphic belts revisited: Gondwana Research, v. 18, p. 46–59, https://doi.org/10.1016/j.gr.2009.11.004.

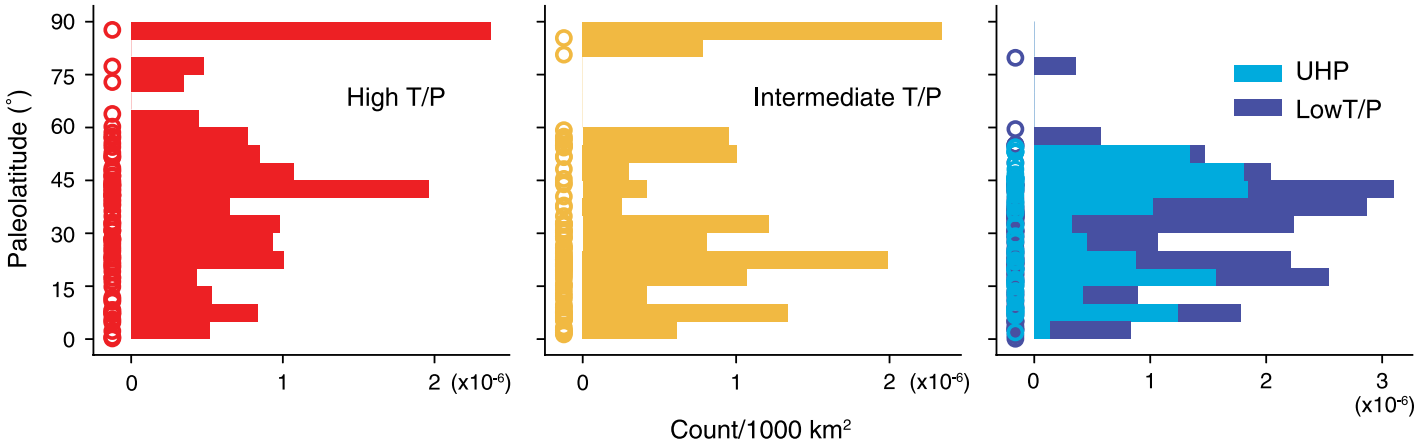

Figure 4. Histogram of paleolatitudes of metamorphic occurrences over the past 1 b.y. by thermobaric ratio (temperature/pressure [*T/P*]) type. Occurrences were normalized to surface area of 5° latitudinal bands. UHP—ultrahigh pressure.

Brown, M., and Johnson, T., 2019a, MSA Presidential Address: Metamorphism and the evolution of subduction on Earth: The American Mineralogist, v. 104, p. 1065–1082, https://doi.org/10.2138/am-2019-6956.

Brown, M., and Johnson, T.E., 2019b, Time's arrow, time's cycle: Granulite metamorphism and geodynamics: Mineralogical Magazine, v. 83, p. 323–338, https://doi.org/10.1180/mgm.2019.19.

Brown, M., Johnson, T., and Gardiner, N. J., 2020, Plate tectonics and the Archean Earth: Annual Review of Earth and Planetary Sciences, v. 48, p. 291–320, https://doi.org/10.1146/annurev-earth-081619-052705.

Chowdhury, P., Chakraborty, S., Gerya, T.V., Cawood, P.A., and Capitanio, F.A., 2020, Peel-back controlled lithospheric convergence explains the secular transitions in Archean metamorphism and magmatism: Earth and Planetary Science Letters, v. 538, p. 116224, https://doi.org/10.1016/j.epsl.2020.116224.

England, P., 2018, On shear stresses, temperatures, and the maximum magnitudes of earthquakes at convergent plate boundaries: Journal of Geophysical Research: Solid Earth, v. 123, p. 7165–7202, https://doi.org/10.1029/2018JB015907.

Gardiner, N.J., Maidment, D.W., Kirkland, C.L., Bodorkos, S., Smithies, R.H., and Jeon, H., 2018, Isotopic insight into the Proterozoic crustal evolution of the Rudall Province, Western Australia: Precambrian Research, v. 313, p. 31–50, https://doi.org/10.1016/j.precamres.2018.05.003.

Hoffman, P.F., 1991, Did the breakout of Laurentia turn Gondwanaland inside-out?: Science, v. 252, p. 1409–1412, https://doi.org/10.1126/science.252.5011.1409.

Holder, R.M., Viete, D.R., Brown, M., and Johnson, T.E., 2019, Metamorphism and the evolution of plate tectonics: Nature, v. 572, p. 378–381, https://doi.org/10.1038/s41586-019-1462-2.

Hyndman, R.D., Currie, C.A., and Pizzotti, S.P., 2005, Subduction zone backarcs, mobile belts, and orogenic heat: GSA Today, v. 15, p. 4–10, https://doi.org/10.1130/1052-5173(2005)015<4:SZBMBA>2.0.CO;2.

Jamieson, R.A., and Beaumont, C., 2013, On the origin of orogens: Geological Society of America Bulletin, v. 125, p. 1671–1702, https://doi.org/10.1130/B30855.1.

Kirscher, U., Mitchell, R.N., Liu, Y., Nordsvan, A.R., Cox, G.M., Pisarevsky, S.A., Wang, C., Wu, L., Murphy, J.B., and Li, Z.X., 2021, Paleomagnetic constraints on the duration of the Australia-Laurentia connection in the core of the Nuna supercontinent: Geology, v. 49, p. 174–179, https://doi.org/10.1130/G47823.1.

Lenardic, A., 2018, The diversity of tectonic modes and thoughts about transitions between them: Philosophical Transactions of the Royal Society, A, v. 376, p. 20170416, https://doi.org/10.1098/rsta.2017.0416.

Li, Z.X., Mitchell, R.N., Spencer, C.J., Ernst, R., Pisarevsky, S.A., Kirscher, U., and Murphy, J.B., 2019, Decoding Earth's rhythm: Modulation of supercontinent cycles by longer superocean episodes: Precambrian Research, v. 323, p. 1–5, https://doi.org/10.1016/j.precamres.2019.01.009.

Liu, Y., Li, Z.X., Pisarevsky, S., Kirscher, U., Mitchell, R.N., and Stark, J.C., 2018, Palaeomagnetism of the 1.89 Ga Boonadgin dykes of the Yilgarn craton: Possible connection with India: Precambrian Research, v. 329, p. 211–223, https://doi.org/10.1016/j.precamres.2018.05.021.

Martin, E.L., Spencer, C.J., Collins, W.J., Thomas, R.J., Macey, P.H., and Roberts, N.M.W., 2020, The core of Rodinia formed by the juxtaposition of opposed retreating and advancing accretionary orogens: Earth-Science Reviews, v. 211, 103413, https://doi.org/10.1016/j.earscirev.2020.103413.

Matthews, K.J., Maloney, K.T., Zahirovic, S., Williams, S.E., Seton, M., and Muller, R.D., 2016, Global plate boundary evolution and kinematics since the late Paleozoic: Global and Planetary Change, v. 146, p. 226–250, https://doi.org/10.1016/j.gloplacha.2016.10.002.

Merdith, A.S., Williams, S.E., Collins, A.S., Tetley, M.G., Mulder, J.A., Blades, M.L., Young, A., Armistead, S.E., Cannon, J., Zahirovic, S., and Müller, R.D., 2021, Extending full-plate tectonic models into deep time: Linking the Neoproterozoic and the Phanerozoic: Earth Science Reviews, v. 214, 103477, https://doi.org/10.1016/j.earscirev.2020.103477.

Mitchell, R.N., Zhang, N., Salminen, J., Liu, Y., Spencer, C.J., Steinberger, B., Murphy, J.B., and Li, Z.X., 2021, The supercontinent cycle: Nature Reviews Earth & Environment, v. 2, p. 358–374, https://doi.org/10.1038/s43017-021-00160-0.

Sobolev, S.V., and Brown, M., 2019, Surface erosion events controlled the evolution of plate tectonics on Earth: Nature, v. 570, p. 52–57, https://doi.org/10.1038/s41586-019-1258-4.

Spencer, C.J., Mitchell, R.N., and Brown, M., 2021, Enigmatic mid-Proterozoic orogens: Hot, thin, and low: Geophysical Research Letters, v. 48, e2021GL093312, https://doi.org/10.1029/2021GL093312.

Tang, M., Chu, X., Hao, J., and Shen, B., 2021, Orogenic quiescence in Earth's middle age: Science, v. 371, p. 728–731, https://doi.org/10.1126/science.abf1876.

Wan, B., Wu, F., Chen, L., Zhao, L., Liang, X., Xiao, W., and Zhu, R., 2019, Cyclical one-way continental rupture-drift in the Tethyan evolution: Subduction-driven plate tectonics: Science China, v. 62, p. 2005–2016, https://doi.org/10.1007/s11430-019-9393-4.

Wan, B., Yang, X., Tian, X., Yuan, H., Kirscher, U., and Mitchell, R.N., 2020, Seismological evidence for the earliest global subduction network at 2 Ga: Science Advances, v. 6, eabc5491, https://doi.org/10.1126/sciadv.abc5491.

Wang, C., Mitchell, R.N., Murphy, J.B., Peng, P., and Spencer, C.J., 2021, The role of megacontinents in the supercontinent cycle: Geology, v. 49, p. 402–406, https://doi.org/10.1130/G47988.1.

Yan, L.L., and Zhang, K.J., 2019, Is exhumation of UHP terranes limited to low latitudes?: Journal of Geodynamics, v. 130, p. 41–56, https://doi.org/10.1016/j.jog.2019.06.004.

Zhao, G., Cawood, P.A., Wilde, S.A., and Sun, M., 2002, Review of global 2.1–1.8 Ga orogens: Implications for a pre-Rodinia supercontinent: Earth-Science Reviews, v. 59, p. 125–162, https://doi.org/10.1016/S0012-8252(02)00073-9.

Zhao, P., He, J., Deng, C., Chen, Y., and Mitchell, R.N., 2021, Early Neoproterozoic (870–820 Ma) amalgamation of the Tarim craton (northwestern China) and the final assembly of Rodinia: Geology, v. 49, p. 1277–1282, https://doi.org/10.1130/G48837.1.

Printed in USA